A high-performance aptasensor for mercury(II) based on the formation of unique ternary structure of aptamer-Hg^{2+}-neutral red

Cai Gao, Qingxiang Wang*, Feng Gao, Fei Gao

College of Chemistry and Environment, Fujian Provincal Key Laboratory of Morden Analytical Science and Separation Technology, Minnan Normal University, Zhangzhou, 363000, P. R. China. Fax: +86-596-2520035; Tel: +86-596-2591445; E-mail: axiang236@126.com

Electronic Supplementary Information

(Including Sensing mechanism of the aptasensor, Experimental details, Aptasensor fabrication characterization, surface density determination of MSA, Test condition optimization, and Supplementary figures/tables)

Description on the working principle of the proposed aptasensor

The working principle for the proposed Hg^{2+} sensor is based on the structure-switching of MSA upon binding to Hg^{2+} and the formation of ternary MSA-Hg^{2+}-NR complex. Figure 1 depicts the main concept of fabrication and analytical process of the designed sensor. First, the thiol-modified 36-mer MSA probe with 22 thymine bases was assembled on the AuE surface through the Au–S bond. Followed by, the electrode was treated with MCH to passivate the uncovered active sites on AuE, and meanwhile to make the MSA strands standing up to achieve the higher reactivity with the analytes. When Hg^{2+} was absent in the test solution, MSA showed a single-stranded and random coil structure, and NR could not interact with MSA. As a result, no electrochemical response could be observed on the sensor. However, when the Hg^{2+} ions were

present and captured by the MSA layer through T-Hg^{2+}-T coordination chemistry, the random coil structured MSA on the electrode surface was transformed to the folded hairpin-like double helix structure. Then when the electrode was immersed in NR solution, the electroactive aromatic molecules of NR inserted into the space between the adjacent T-Hg^{2+}-T pairs that embedded in the folded MSA and meanwhile coordinated with the Hg^{2+} through its free amino groups. Thus the NR was tightly captured by the sensing film, and the electrochemical signal of NR was observed.

Experimental details:

(1) Materials and Reagents

The thiolated MSA sequence is as follows:[1] 5'-SH-$(CH_2)_6$-TCT TTC TTC TTT CTT CCC CCC TTG TTT GTT GTT TGT-3', which was synthesized by Sangon Biotechnology Co., Ltd. (Shanghai, China). L-cysteine (L-cys) was purchased from Sinopharm Chemical Reagent Co., Ltd. (Shanghai, China). 6-Mercapto-1-hexanol (MCH) and NR were bought from Chemical Reagents Co., Ltd. (Wenzhou, China). All the metal salts (NaCl, $CaCl_2$, $MgCl_2 \cdot 6H_2O$, $ZnCl_2$, $NiCl_2 \cdot 6H_2O$, $HgCl_2$, $AgNO_3$, $CuSO_4 \cdot 5H_2O$, $CdCl_2 \cdot 2.5H_2O$, $MnSO_4 \cdot H_2O$, $Co(CH_3COO)_2 \cdot 4H_2O$, KNO_3, $Pb(NO_3)_2$) used in this study were provided by Xilong Chemical Co., Ltd. (Guangdong, China) and used directly without further purification. The other reagents such as tris(hydroxymethyl) aminomethane (Tris), tris(2-carboxyethyl) phosphine hydrochloride (TCEP) and $K_3Fe(CN)_6$/$K_4Fe(CN)_6$ were of analytical reagent grades and purchased commercially. Doubly distilled water (DDW) was used throughout the experiments.

The stock solutions of MSA (10 μM) was prepared with IB buffer solution (25 mM Tris-HCl, 100 mM NaCl, 100 mM $MgCl_2$ and 10 mM TCEP, pH 8.2) and kept frozen before use. Britton-Robinson (B-R) buffer solution was used as the supporting electrolyte for the electrochemical measurements of NR. Prior to measurements, all the electrolytes were purged with nitrogen. Phosphate buffer solution (25 mM) was prepared by mixing an appropriate content of 0.2 M NaH_2PO_4 and 0.2 M Na_2HPO_4.

(2) Instruments

Electrochemical measurements were carried out on a CHI 650C electrochemical workstation

(Chenhua Instrument Co., LTD, Shanghai, China) at room temperature. A three-electrode system consist of a bare or modified gold electrode (AuE, Geometric area (A)=3.14×10^{-2} cm^2) as the working electrode, a platinum wire as the counter electrode, and an Ag/AgCl (3 M KCl) as the reference electrode. The pH of all solutions was measured on a Model pHs25 digital acidometer (Shanghai Leici Factory, Shanghai, China). The ICP-MS detection of Hg^{2+} was performed on an Agilent model 7500cx analyzer (Agilent Technologies, Tokyo, Japan). The absorption spectra were recorded on a UV-1800 PC spectrophotometer (Shanghai Meipuda, Shanghai, China).

(3) Fabrication of the sensor

Prior to fabrication, the bare AuE was polished with 1.0 μm, 0.3 μm, and 0.05 μm alumina slurry, followed by ultrasonic cleaning in DDW, ethanol and DDW, in turn. Then the freshly polished electrode was dipped in Piranha solution (98%H_2SO_4/30%H_2O_2, 7:3, V/V) for 30 min and then electrochemically scanned between -0.2 and +1.5 V in 0.5 M H_2SO_4 until stable voltammetric curves were obtained. After that, the electrode was rinsed with DDW and dried with nitrogen stream and then immediately dipped in 0.1 μM MSA solution at 4 ℃ for 24 h. Following rinsing with DDW to remove the non-specifically adsorbed DNA, the MSA modified electrode (MSA/AuE) was fabricated. Finally, the MSA/AuE was incubated in 1 mM MCH for 2 h to cover the rest surface, and the obtained electrode was denoted as MCH-MSA/AuE.

(4) Electrochemical determination of Hg^{2+}

To detect Hg^{2+}, the MCH-MSA/AuE was initially incubated in 200 μL solution containing desired concentration of Hg^{2+} for 100 min at room temperature. Then the electrode was immersed into 25 mM PBS solution for 10 min with gently shaking to remove the nonspecifically adsorbed Hg^{2+} ions. Subsequently, the Hg^{2+} adsorbed electrode (Hg^{2+}/MCH-MSA/AuE) was immersed in 1.4 mM NR solution for 1 h to sufficiently accumulate the electroactive NR molecules. After rinsing with PBS, the NR assembled electrode (NR/Hg^{2+}/MCH-MSA/AuE) was electrochemically measured in 40 mM B-R (pH 7.0) buffer solution through cyclic voltammetry (CV) and differential pulse voltammetry (DPV). The control experiments were carried out through the same

method except replacing the Hg^{2+} with the other metal ions.

Safety considerations: As the Piranha solution, Hg^{2+} and most of the other tested metal ions are highly toxic and have adverse effects on human health, all the experiments involving these materials should be performed with protective gloves. The waste solutions containing heavy metal ions should be collectively reclaimed after test to avoid the environment pollution.[2]

(5) DNA surface density determination

The DNA surface density was determined using a typical CC technology that has reported by Steel et al.[3] It is accorded that $[Ru(NH_3)_6]^{3+}$ cations as counter ions can bind to anionic phosphate of DNA strands in a stoichiometric approach, thereby allowing the quantitative analysis of the loading amount of DNA. In the experiment, the charge (Q), as a function of time (t) is given by the following integrated Cottrell expression:

$$Q = \frac{2nFAD_0^{1/2}C_0^*}{\pi^{1/2}}t^{1/2} + Q_{dl} + nFA\Gamma_0 \qquad (1)$$

Where n is the number of electrons per molecule for reduction, F the Faraday constant (C/mol), A the electrode area (cm^2), D_0 the diffusion coefficient ($cm^2\ s^{-1}$), C^*_0 the bulk concentration (mol cm^{-2}), Q_{dl} the capacitive charge (C), and $nFA\Gamma_0$ is the charge from the reduction of adsorbed redox markers. The intercept at $t = 0$ is the sum of the double layer charging and the surface excess terms. Then when the double layer capacitance is assumed to be approximately equal in measurements with and without $[Ru(NH_3)_6]^{3+}$ [4] and Q_{dl} for the fixed voltage step is constant, $nFA\Gamma_0$ can be achieved by measuring the difference in intercepts of the two cases, and the DNA surface density can be further determined by the following equation:

$$\Gamma_{DNA} = \Gamma_0\left(\frac{z}{m}\right)N_A \qquad (2)$$

Where Γ_{DNA} is the probe surface density (strands cm^{-2}), m the number of phosphate groups on the probe DNA, z the charge on the redox molecule, and N_A the Avogadro's number.

Electrochemical characterization on the fabrication of the sensor

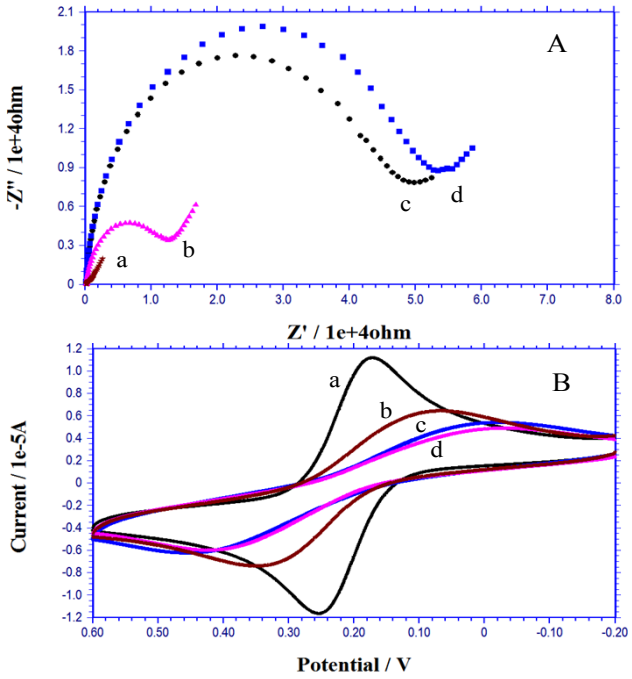

Fig. S1 (A) Nyquist plots and (B) CVs of 1 mM $[Fe(CN)_6]^{3-/4-}$ solution containing 0.1 M KCl at bare AuE (a), MSA/AuE (b) and MCH-MSA/AuE before (c) and after incubation in Hg^{2+} solution (d) for 100 min. The concentration of Hg^{2+} was 8.5×10^{-9} M.

The stepwise fabrication process of the sensor was electrochemically characterized using $[Fe(CN)_6]^{3-/4-}$ as the redox probe, and the electrochemical impendence spectroscopy (EIS) and CV results are showed in Fig. S1-A and Fig. S1-B, respectively. In EIS, the electron transfer resistance (R_{ct}) was directly estimated from the semicircle diameter at the high frequency region.[5] From the Nyquist plots, one could observe that the bare AuE displayed a small semicircle at the high frequency region (curve a), indicating a low electron transfer resistance on the bare AuE. After MSA was self-assembled onto the surface of AuE, the R_{ct} was increased markedly (curve b), which suggested that MSA had been successfully assembled on AuE. This was because the negatively charged phosphate backbone on MSA hindered the electron transfer between the electrode and the electroactive $[Fe(CN)_6]^{3-/4-}$ ions. Subsequently, when MSA/AuE was treated with MCH, the R_{ct} value was further increased (curve c) since the net negative dipole of the alcohol terminus on the gold surface further repelled $[Fe(CN)_6]^{3-/4-}$.[6] After the MCH-MSA/AuE was incubated with Hg^{2+}, a further increase of R_{ct} was observed (curve d), which could be

explained by the increase of steric-hindrance of the formed hairpin-like structure to the negatively charged $[Fe(CN)_6]^{3-/4-}$ ions. This also indicated that the aptasensor of MCH-MSA/AuE is responsive to the Hg^{2+}.

As a further proof, CV responses of $[Fe(CN)_6]^{3-/4-}$ at different modified electrodes were also investigated (see Fig. S1-B of the Supporting Information), and the results were in good agreement with those from above EIS studies.

Condition optimization of the aptasensor

In order to obtain the optimal sensing performance of the sensor, some experimental conditions such as the reaction time between Hg^{2+} and MSA, the accumulation time and the accumulation concentration of NR were optimized. The reaction time between Hg^{2+} and MCH-MSA/AuE was investigated by EIS. Fig. S2-A shows the relationship of R_{ct} values versus the reaction time ($t_{Hg}{}^{2+}$). It was observed that with the increase of reaction time, the R_{ct} value increased gradually, indicating that more and more Hg^{2+} induced hairpin structured DNA had been formed on the electrode surface. When the time was upon 100 min, the R_{ct} became a constant, which was an indication of the binding equilibrium between MSA and Hg^{2+}. Therefore, 100 min was selected as the optimal binding time of Hg^{2+} in this work.

In addition, it could be imagined that with the increase of accumulation time of NR (t_{NR}) on Hg^{2+}/MCH-MSA/AuE, the amount of NR adsorbed on electrode surface would be increased, and consequently the electrochemical signal of NR would be enhanced. Therefore in this work the effect of accumulation time of Hg^{2+}/MCH-MSA/AuE in NR solution on the electrochemical response was also probed. The results proved that with the increase t_{NR}, the oxidation peak currents (I_{pa}) corresponding to the oxidation of NR increased gradually. When the time was up to 60 min (Fig. S2-B), the I_{pa} value reached to the maximum value, suggesting that the binding of NR on Hg^{2+}/MCH-MSA/AuE had been saturated. Thus, 60 min was chosen as the optimal accumulation time for NR. The effect of the accumulation concentration (C_{NR}) of NR on the response signal of the sensor showed that the I_{pa} values of NR enhanced with the increase of C_{NR} in the range from 0.2 mM to 1.8 mM, and then tended to be constant when the concentration was 1.4 mM (Fig. S2-C). So, 1.4 mM was selected as the optimal accumulation concentration in the following studies.

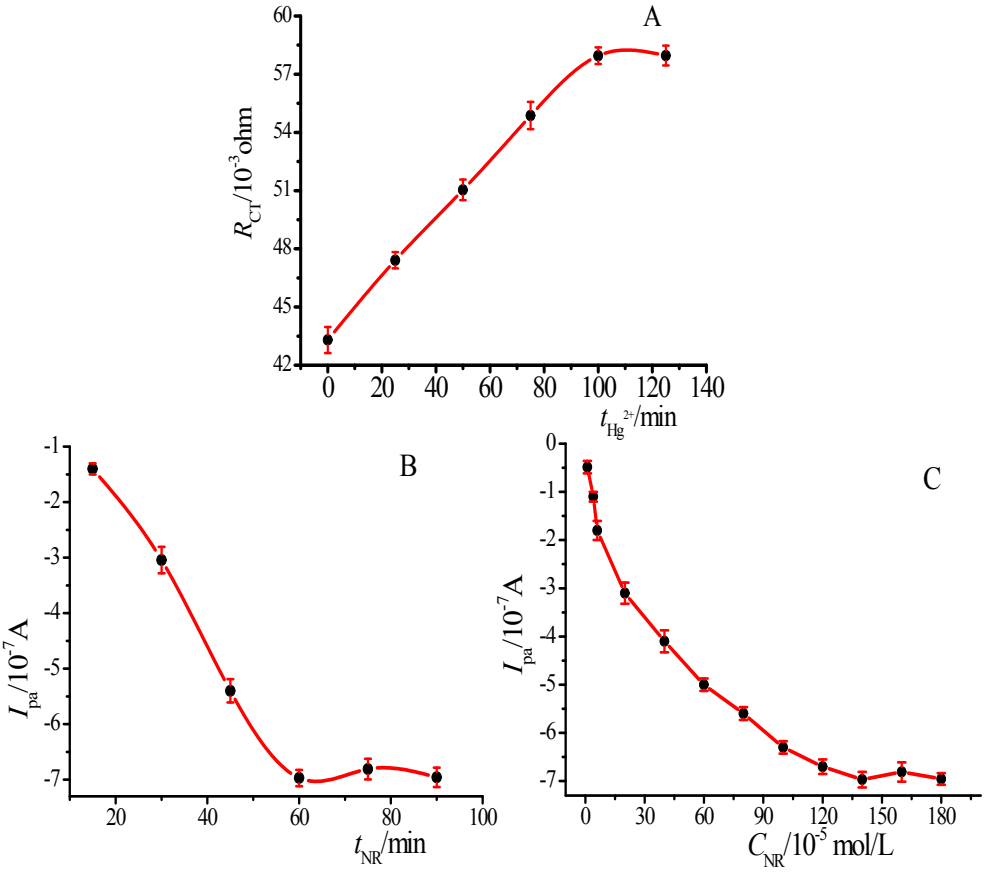

Fig. S2. (A) Effect of reaction time of Hg^{2+} ($t_{Hg^{2+}}$) on the R_{ct} values at the MCH-MSA/AuE. (B) Relationships of peak currents (I_{pa}) versus pre-accumulation time (t_{NR}) and (C) pre-accumulation concentration (C_{NR}) of NR on Hg^{2+}/MCH-MSA/AuE. The concentrations of Hg^{2+} used in all assays are 8.5×10^{-9} M.

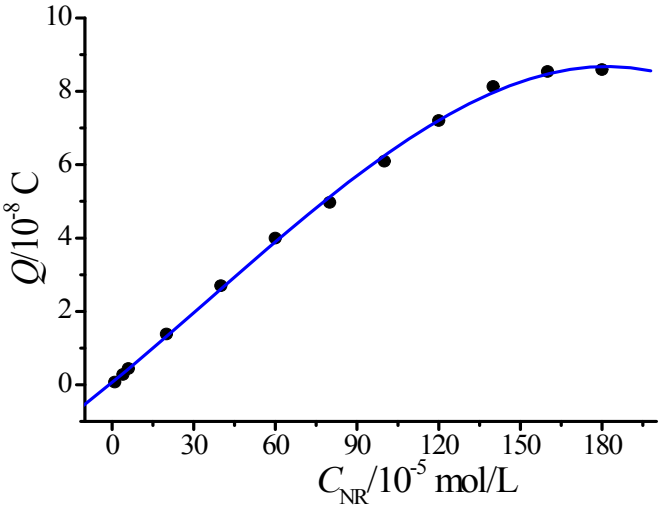

Fig. S3. Relationship of the coulometric charge (Q) versus the C_{NR}.

MSA surface density of the aptasensor

Fig. S4 is the typical CC curves of MCH/MSA/Au in Tris-HCl buffer solution without (curve a) and with 50 μM $[Ru(NH_3)_6]^{3+}$ (curve b). The surface density of the probe DNA can be obtained with the assumption that the redox active $[Ru(NH_3)_6]^{3+}$ molecule stoichiometrically binds to the anionic phosphate backbone of DNA. The surface densities of the probe DNA can then be calculated from the redox charges of $[Ru(NH_3)_6]^{3+}$ according to chronocoulometric methods. Then, from the intercept difference of $Q \sim t^{1/2}$ between curve b and curve a, the value of $nFA\Gamma_0$ corresponding to the electroactive $[Ru(NH_3)_6]^{3+}$ electrostatically bound to the probe DNA was determined to be 6.88 μC.

Thus, based on Equation (2), the value of Γ_{DNA} was determined to be 3.78×10^{12} molecules cm^{-2} was achieved and the binding ratio of NR to Hg^{2+}-MSA, Γ_{NR}: Γ_{MSA}, was determined to be 7.9. This meant that each Hg^{2+}-MSA strand adsorbed 8 NR molecules on average.

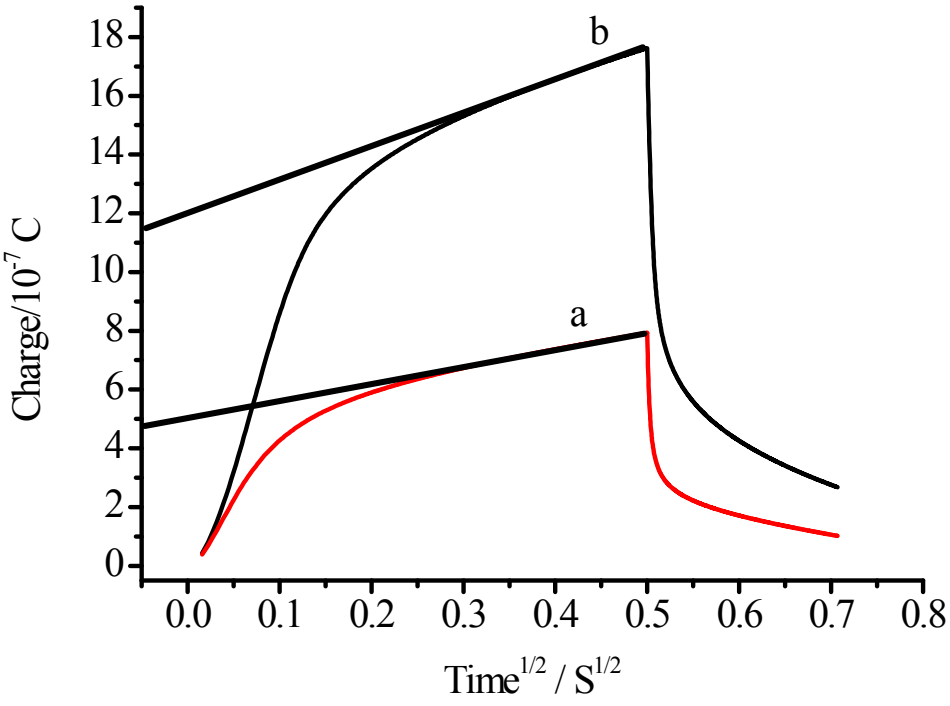

Fig. S4. Chronocoulometric response curves for MCH (curve a) and MSA/MCH (curve b) modified electrodes in the absence and presence of 50 μM $[Ru(NH_3)_6]^{3+}$

Selectivity of the aptasensor.

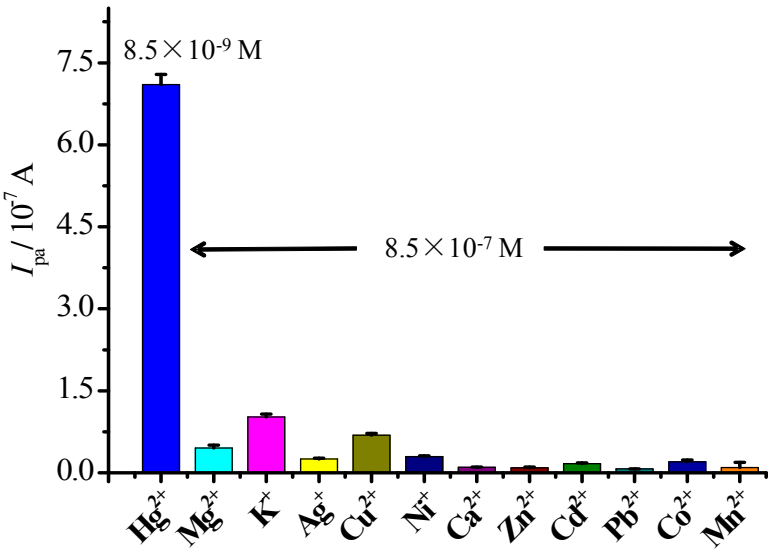

Fig. S5. DPV signal (ΔI_{pa}) of the sensor in response to Hg^{2+} ions (8.5×10^{-9} M) and other various metal ions (8.5×10^{-7} M).

Regenerability, reproducibility and stability of aptasensor

The stability of the developed sensor was also investigated by keeping the electrode in the fridge at 4 °C and recording its current response each day. In the first week, only 7.5% loss in the current signal was observed, showing high stability of the sensor.

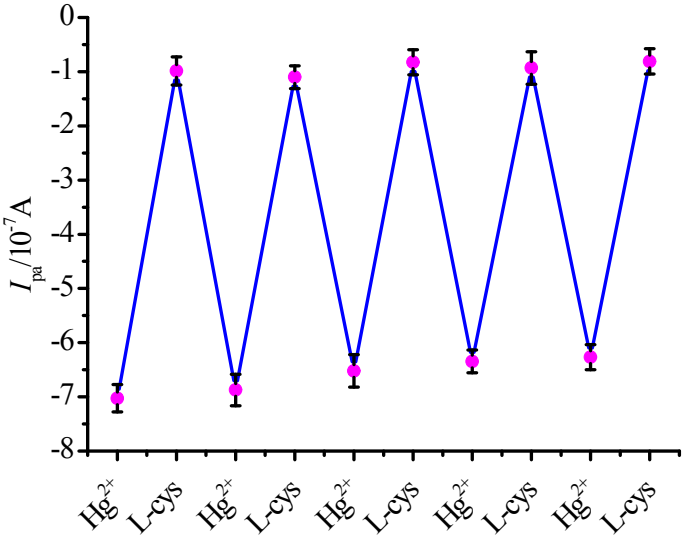

Fig. S6. Typical DPV peak currents (I_{pa}) of the sensor five response regeneration runs. The concentration of Hg^{2+} is 8.5×10^{-9} M.

Table S1 Comparison of the analytical performance of MSA-based electrochemical Hg^{2+} sensors

Sensing layer	Detection methods	Signaling molecules	Covalent pre-labeling (+) or not (-)	Linear range (nM)	LOD (nM)	Refs.
MSA/cMSA/AuE	DPV	ferrocene	+	0.1~ 5000	0.06	5
MSA/cMSA /PDA-RGO/GCE	DPV	$[Ru(NH_3)_6]^{3+}$	-	8 ~ 100	5	7
poly$(T)_{30}$/AuE	EIS	$[Fe(CN)_6]^{3-/4-}$	-	1 ~ 1×10^6	0.1	8
MSA-AuNPs/cMSA/AuE	CV	$[Ru(NH_3)_6]^{3+}$	-	-	10	9
MSA/AuE	DPV	ferrocene	+	5 ~ 1000	2.5	10
MSA/AuE	DPV	neutral red	-	0.027~ 8.5	0.0015	This work

Note: cMSA: DNA fragment complementary to MSA; PDA-RGO: polydopamine-capped reduced graphene oxide; MSA-AuNPs: MSA labeled Au nanoparticles.

Table S2 Determination of Hg^{2+} in water samples using the developed aptasensor and ICP-MS[a].

Water sample	Developed aptasensor (nM)	ICP-MS method (nM)	Relative deviation[b]
Pure drinking water	nondetectable	nondetectable	—
River water 1	39.98±5.12	42.09±4.91	-5.01%
River water 2	40.23±4.25	37.35±3.28	7.71%
Tap water 1	14.01±4.21	15.21±5.73	-7.89%
Tap water 2	15.74±3.70	16.92±5.01	-6.97%

[a]All values were obtained as average of five repetitive determinations plus standard deviation.
[b]Relative deviations were obtained by dividing the difference between the results using ICP-MS and the developed new aptasensor.

References

1. Y. Wu, S. Zhan, L. Xu, W. Shi, T. Xi, X. Zhan and P. Zhou, *Chem. Commun*. 2011, **47**, 6027–6029.
2. T. Li, S. Dong and E. Wang, *Anal. Chem*. 2009, **81**, 2144–2149.
3. A. B. Steel, T. M. Herne and M. J. Tarlov, Anal. Chem., 1998, 70, 4670–4677.

4. J. Zhang, S. Song, L. Zhang, L. Wang, H. Wu, D. Pan, C. Fan, J. Am. Chem. Soc. 128 (2006) 8575−8580.
5. D. Wu, Q. Zhang, X. Chu H. Wang, G. Shen and Yu R. *Biosens. bioelectron.*, 2010, **25**, 1025–1031.
6. Z. S. Wu, C. R. Chen, G. L. Shen and R. Q. Yu, *Biomaterials*, 2008, **29**, 2689–2696.
7. Y. Zhang, H. Zhao, Z. Wu, Y. Xue, X. Zhang, Y. He, X. Li and Z. Yuan, *Biosens. Bioelectron.*, 2013, **48**, 180–187.
8. R. Cao, B. Zhu, J. Li and D. Xu, *Electrochem. Commun.*, 2009, **11**, 1815–1818.
9. P. Miao, L. Liu, Y. Li and G. Li, *Electrochem. Commun*., 2009, **11**, 1904–1907.
10. J. Zhuang, L. Fu, D. Tang, M. Xu, G. Chen and H. Yang, *Biosens. Bioelectron.* 2013, **39**, 315–319.